



# MIT Open Access Articles

## *Reactive nitrogen species regulate autophagy through ATM-AMPK-TSC2-mediated suppression of mTORC1*

The MIT Faculty has made this article openly available. **Please share** how this access benefits you. Your story matters.

<b>Citation</b>	Tripathi, D. N., R. Chowdhury, L. J. Trudel, A. R. Tee, R. S. Slack, C. L. Walker, and G. N. Wogan. "Reactive Nitrogen Species Regulate Autophagy through ATM-AMPK-TSC2-Mediated Suppression of mTORC1." <i>Proceedings of the National Academy of Sciences</i> 110, no. 32 (August 6, 2013): E2950–E2957.
<b>As Published</b>	<a href="http://dx.doi.org/10.1073/pnas.1307736110">http://dx.doi.org/10.1073/pnas.1307736110</a>
<b>Publisher</b>	National Academy of Sciences (U.S.)
<b>Version</b>	Final published version
<b>Accessed</b>	Tue Sep 11 15:30:11 EDT 2018
<b>Citable Link</b>	<a href="http://hdl.handle.net/1721.1/85913">http://hdl.handle.net/1721.1/85913</a>
<b>Terms of Use</b>	Article is made available in accordance with the publisher's policy and may be subject to US copyright law. Please refer to the publisher's site for terms of use.
<b>Detailed Terms</b>	

# Reactive nitrogen species regulate autophagy through ATM-AMPK-TSC2-mediated suppression of mTORC1

Durga N. Tripathi<sup>a,1</sup>, Rajdeep Chowdhury<sup>b,1</sup>, Laura J. Trudel<sup>c</sup>, Andrew R. Tee<sup>d</sup>, Rebecca S. Slack<sup>e</sup>, Cheryl Lyn Walker<sup>a</sup>, and Gerald N. Wogan<sup>c,2</sup>

<sup>a</sup>Institute for Biosciences and Technology, Texas A&M Health Science Center, Houston, TX 77030; <sup>b</sup>Birla Institute of Technology and Science (BITS), Pilani Campus, Rajasthan 333031, India; <sup>c</sup>Department of Biological Engineering, Massachusetts Institute of Technology, Cambridge, MA 02139; <sup>d</sup>Institute of Medical Genetics, Cardiff University, Cardiff CF14 4XN, Wales, United Kingdom; and <sup>e</sup>Department of Biostatistics, University of Texas M. D. Anderson Cancer Center, Houston, TX 77030

Contributed by Gerald N. Wogan, April 29, 2013 (sent for review March 4, 2013)

Reactive intermediates such as reactive nitrogen species play essential roles in the cell as signaling molecules but, in excess, constitute a major source of cellular damage. We found that nitrosative stress induced by steady-state nitric oxide (NO) caused rapid activation of an ATM damage-response pathway leading to downstream signaling by this stress kinase to LKB1 and AMPK kinases, and activation of the TSC tumor suppressor. As a result, in an ATM-, LKB1-, TSC-dependent fashion, mTORC1 was repressed, as evidenced by decreased phosphorylation of S6K, 4E-BP1, and ULK1, direct targets of the mTORC1 kinase. Decreased ULK1 phosphorylation by mTORC1 at S757 and activation of AMPK to phosphorylate ULK1 at S317 in response to nitrosative stress resulted in increased autophagy: the LC3-II/LC3-I ratio increased as did GFP-LC3 puncta and acidic vesicles; p62 levels decreased in a lysosome-dependent manner, confirming an NO-induced increase in autophagic flux. Induction of autophagy by NO correlated with loss of cell viability, suggesting that, in this setting, autophagy was functioning primarily as a cytotoxic response to excess nitrosative stress. These data identify a nitrosative-stress signaling pathway that engages ATM and the LKB1 and TSC2 tumor suppressors to repress mTORC1 and regulate autophagy. As cancer cells are particularly sensitive to nitrosative stress, these data open another path for therapies capitalizing on the ability of reactive nitrogen species to induce autophagy-mediated cell death.

signal transduction | cancer therapy

**A**utophagy is a self-digestion process by which a eukaryotic cell degrades and recycles aggregate-prone proteins, macromolecules, and organelles. During autophagy, cytoplasmic contents are sequestered in double-membrane bound vesicles called autophagosomes and delivered to lysosomes for degradation, thereby allowing cells to eliminate and recycle the contents (1–3). Autophagy participates in both prosurvival (recycling of cellular building blocks) and prodeath (excess catalysis) pathways. A comprehensive understanding of signaling pathways that regulate autophagy holds great promise for new therapeutic opportunities by opening the possibility to compromise prosurvival autophagic pathways that enable tumor cells to evade therapy, or by promoting prodeath autophagic pathways to kill cancer cells.

The classical pathway regulating autophagy in mammalian cells involves the serine/threonine kinase, mammalian target of rapamycin (mTOR). Active mTOR kinase in the mTORC1 complex phosphorylates and inhibits ULK1, a key proautophagy adapter involved in nucleation of the autophagophore membrane. Inactivation of mTORC1, either pharmacologically with rapamycin or via activation of the tuberous sclerosis complex (TSC) tumor suppressor, leads to downstream dephosphorylation events, including loss of ULK1 phosphorylation at S757. The TSC1/2 heterodimer is itself regulated by upstream kinases, including the AMP-activated protein kinase (AMPK), which regulates several metabolic processes and activates the TSC to repress mTORC1 under conditions of energy stress (4–6). AMPK also

directly regulates autophagy by phosphorylating and activating ULK1 at S317 (7).

Nitric oxide (NO) is a pleiotropic regulator, critical to numerous biological processes extending from its role as a chemical messenger and antibacterial agent to an integral component of the cardiovascular system and immune response to pathogens (8). NO has also been documented to play both promotional and inhibitory roles in cancer etiology. NO is produced endogenously by tumor cells of various histogenetic origins and has been associated with tumor proliferation and resistance to anticancer drugs. Although cancer cells may maintain endogenous NO at elevated levels that facilitate tumor growth, this strategy carries a survival liability, as high levels of NO can cause cytostasis or cytotoxicity (9). Thus, cancer cells may be more sensitive to NO-induced nitrosative stress, which could potentially provide a therapeutic avenue for modulating nitrosative stress to induce cell death. However, understanding at the molecular level regarding how NO participates in regulation of either prosurvival or prodeath autophagic pathways is limited.

Recently, a novel signaling pathway involving activation of ATM to suppress mTORC1 in response to oxidative damage was identified (10). In the study reported here, we demonstrate that NO engages this pathway to suppress mTORC1 and promote autophagy. In response to nitrosative stress induced by steady-state exposure to NO, ATM is activated, signaling to AMPK via LKB1 to activate the TSC tumor suppressor and suppress mTORC1. Concomitant with suppression of mTORC1, autophagy is induced, accompanied by loss of cell viability. Our data provide

## Significance

**NO exposure triggered an ATM-mediated damage response in breast cancer cells involving activation of the LKB1 and TSC2 tumor suppressors, repression of mTORC1, ULK phosphorylation, and increased autophagic flux. The associated loss of cell viability indicates that autophagy can function as a cytotoxic response to nitrosative stress in tumor cells. Collectively, the data identify a nitrosative-stress signaling pathway that regulates autophagy. A more comprehensive understanding of signaling pathways regulating autophagy holds promise for developing new therapeutic approaches compromising prosurvival autophagic pathways that enable tumor cells to evade therapy, or promoting prodeath autophagic pathways that kill cancer cells.**

Author contributions: D.N.T., R.C., L.J.T., C.L.W., and G.N.W. designed research; D.N.T., R.C., and L.J.T. performed research; D.N.T., R.C., L.J.T., A.R.T., R.S.S., C.L.W., and G.N.W. analyzed data; D.N.T., R.C., L.J.T., R.S.S., C.L.W., and G.N.W. wrote the paper; and A.R.T. developed the model in Fig 5.

The authors declare no conflict of interest.

<sup>1</sup>D.N.T. and R.C. contributed equally to this work.

<sup>2</sup>To whom correspondence should be addressed. E-mail: wogan@mit.edu.

This article contains supporting information online at [www.pnas.org/lookup/suppl/doi:10.1073/pnas.1307736110/-DCSupplemental](http://www.pnas.org/lookup/suppl/doi:10.1073/pnas.1307736110/-DCSupplemental).

strong evidence that NO regulates autophagy, with implications both for understanding the physiological role of NO-induced signaling and the development of therapies that can modulate nitrosative stress to kill cancer cells.

## Results

**Steady-State Exposure to Nitric Oxide Decreases Survival of MCF-7 Cells.** MCF-7 breast cancer cells were exposed to increasing NO cumulative doses from 0 to 2,488  $\mu\text{M}\cdot\text{min}$ . This dose escalation was achieved by exposing cells in a reactor to a steady-state concentration of 11  $\mu\text{M}$  NO for increasing lengths of time from 0 to 280 min. Twenty-four hours postexposure, cells showed decreased cell viability, compared with untreated controls, ranging from 27% to 40% after exposure to cumulative doses of NO from 1,244  $\mu\text{M}\cdot\text{min}$  (140 min) to 2,488  $\mu\text{M}\cdot\text{min}$  (280 min), respectively (Fig. 1A). Treatment of control cells with 5%  $\text{CO}_2$ :21%  $\text{O}_2$ :74%  $\text{N}_2$  had no effect on cell viability. Importantly, the following evidence showed that decreased cell viability was not associated with increased apoptosis or programmed necrosis,

suggesting rather that it was due to alternative cell death pathway(s): AnnexinV/PI staining and flow cytometry (Fig. 1B); cleavage of poly (ADP-Ribose) polymerase (PARP, a marker for apoptosis) (Fig. 1C); and exposures to NO in the presence or absence of the caspase inhibitor Z-VAD-FMK or the necroptosis inhibitor necrostatin-1 (Fig. S1 A, B, and C).

### Nitric Oxide Suppresses mTORC1 Signaling and Induces Autophagy.

We observed that the same steady-state (11  $\mu\text{M}$ ) NO exposure that induced cell death also suppressed mTORC1 signaling, as observed by reduced phosphorylation of p70/S6 kinase, 4E-BP1 (S6K and 4E-BP1 are direct targets of the mTOR kinase) and phosphorylation of S6 (downstream effector target of S6K) (Fig. 24). Reduction in mTORC1 signaling occurred between 140 and 280 min exposure, at NO doses between 1,244  $\mu\text{M}\cdot\text{min}$  (140 min) and 2,488  $\mu\text{M}\cdot\text{min}$  (280 min). Comparable results were obtained when MCF-7 cells were treated with the NO donor spermine NONOate (SN), which similarly reduced phosphorylation of S6K and S6 in a time-dependent manner, with maxi-

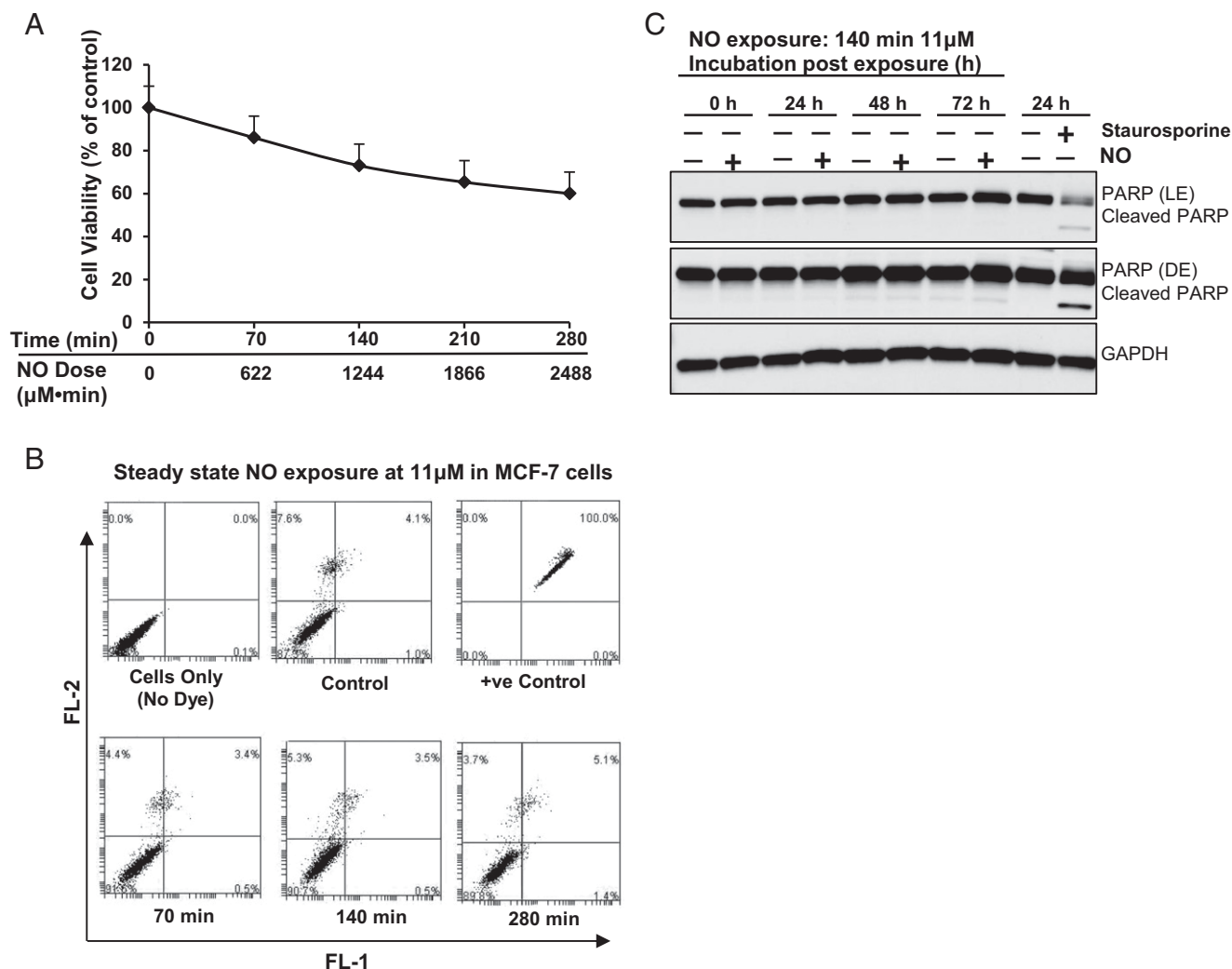


**Fig. 1.** (A) NO exposure leads to decrease in survival of MCF-7 cells. Cell viability was estimated following NO exposure at a steady-state concentration of 11  $\mu\text{M}$  to attain the cumulative doses (622–2,488  $\mu\text{M}\cdot\text{min}$ ) presented on the x axis. Cell viability was measured by WST-1 assay 24 h after NO exposure and expressed as % of control. The data are represented as mean  $\pm$  SD. (B) Steady-state NO exposure did not increase apoptosis in MCF-7 cells as observed by annexin-V staining. Emodin at a dose of 20  $\mu\text{M}$  served as a positive control. (C) Western analysis with PARP antibody shows that exposure of MCF-7 cells to NO is not associated with the activation of PARP. Cells were exposed to NO at a steady-state concentration of 11  $\mu\text{M}$  to attain the cumulative dose of 1,244  $\mu\text{M}\cdot\text{min}$ , and lysates were prepared at 0 h, 24 h, 48 h, and 72 h postexposure. Staurosporine at the dose of 1  $\mu\text{M}$  served as a positive control. LE represents light (short) exposure and DE represents dark (long) exposure of X-ray film.

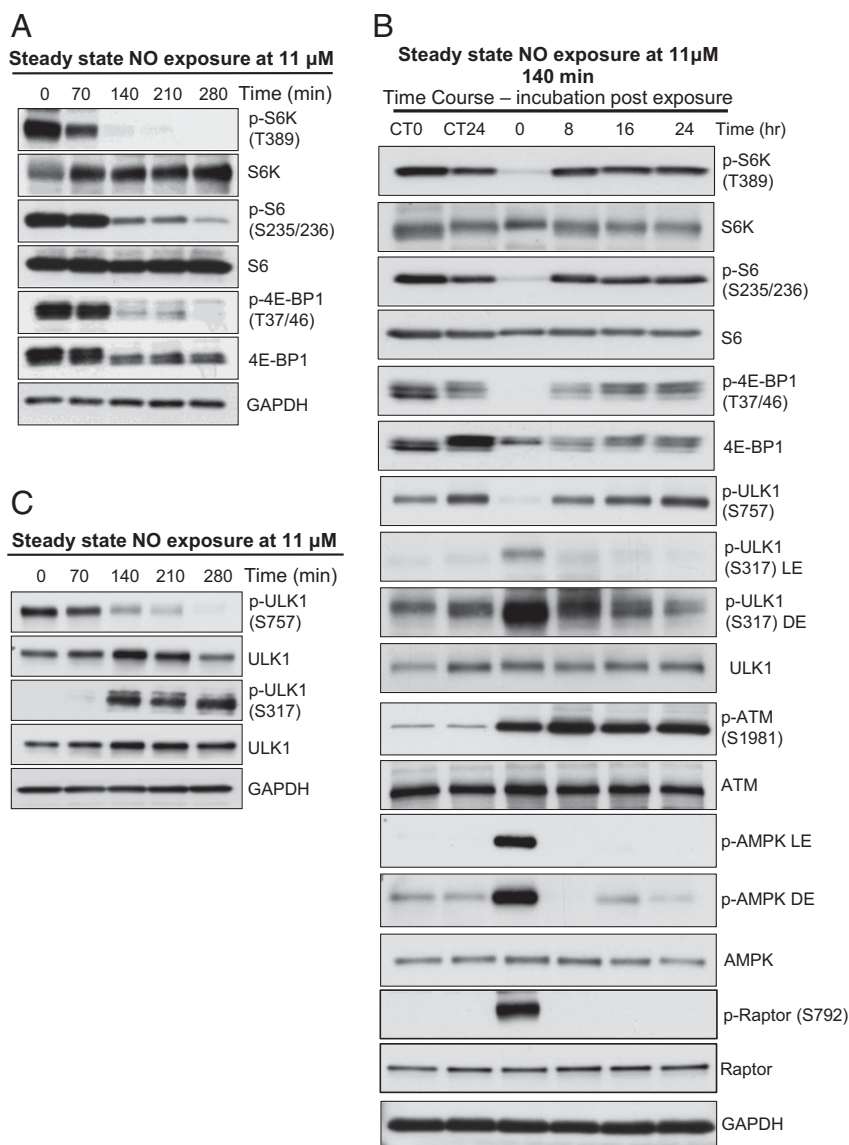


**Fig. 2.** Steady-state NO exposure leads to repression of mTORC1. (A) Western analysis with p-S6K, p-S6, and p-4E-BP1 antibodies shows suppression of mTORC1 in NO-treated MCF-7 cells. (B) Restoration of mTORC1 activity after NO exposure when cells are incubated in normal culture condition. Time course study: cells were exposed to steady-state 11  $\mu$ M NO for 140 min, and lysates were prepared after 0, 8, 16, and 24 h incubation in normal culture condition. Western analysis of p-S6K, p-S6, p-4E-BP1, p-ULK1 (S757), p-ULK1 (S317), p-ATM, p-AMPK, and total protein in MCF-7 cells. (C) Western analysis with p-ULK1 antibody shows decreased phosphorylation of ULK1 at mTORC1 site S757 and increase in phosphorylation of ULK1 at AMPK site S317 in NO-treated MCF-7 cells. CT0 represents control (no NO) at 0 time point, and CT24 represents control at 24 h time point. LE represents light (short) exposure and DE represents dark (long) exposure of X-ray film.

imum inhibition 2–8 h after treatment and return to baseline at 16 h (Fig. S24). A similar rebound to baseline was seen after removal of cells from the NO reactor; suppressed mTORC1 signaling in the presence of NO returned to baseline 8 h after removal from the reactor and remained at baseline for 24 h thereafter (Fig. 2B and Fig. S2B).

mTORC1 is a well-known negative regulator of autophagy. Recent reports indicate that mTORC1 and AMPK have opposing effects on autophagy mediated via phosphorylation of ULK1 at different regulatory sites (7). ULK1 is a key protein required for nucleation of the autophagophore and formation of the autophagosome membrane (11). Under optimal growth conditions, activated mTORC1 inhibits autophagy by direct phosphorylation of Atg13 and Unc-51-like kinase 1 (ULK1) at S757. This phosphorylation inhibits ULK1 kinase activity and subsequent autophagosome formation (12). However, under

conditions of energy stress, AMPK suppresses mTORC1 via TSC and phosphorylates ULK1 at S317, initiating autophagosome formation and autophagy. As shown in Fig. 2B and C, mTORC1 phosphorylation of ULK1 at S757 was inhibited whereas ULK1 phosphorylation at the S317 AMPK site increased in response to NO exposure. In the NO reactor, these changes in ULK1 phosphorylation were induced by exposure to 1,244–2,488  $\mu$ M•min NO (Fig. 2C), and 2–4 h after treatment with SN (Fig. S34).

Concomitant with reduced mTORC1/increased AMPK phosphorylation of ULK1, cells were induced to undergo autophagy as determined using several autophagic markers. Microtubule-associated protein 1A/1B-light chain 3 (LC3-I), the mammalian homolog of the yeast protein Atg8 (Aut7/Apg8p), is conjugated to phosphatidylethanolamine to form LC3-phosphatidylethanolamine conjugate (LC3-II), which is recruited to autophagosomal membranes (13, 14). Exposure of MCF-7 cells to NO



increased the ratios of LC3-II/LC3-I and LC3-II/GAPDH as determined by western analysis (Fig. 3A), indicative of increased autophagosome formation in response to mTORC1 repression. LC3-II to LC3-I ratios and LC3-II to GAPDH ratios remained elevated 24 h after cells were withdrawn from the NO reactor, suggesting that NO-induced autophagy persisted in these cells, possibly due to the continued presence of reactive nitrogen species formed during NO exposure (Fig. 3B).

To confirm that increased autophagosome formation was due to increased autophagic flux, cells were treated with Bafilomycin A1 (BafA1), which blocks lysosomal degradation of autolysosome contents. Efficacy of this treatment was confirmed by an increase in LC3-II levels in response to BafA1, with or without NO treatment (Fig. 3C and Fig. S3B). Similarly, whereas the long-lived protein and autophagy marker p62 decreased in response to NO, treatment with BafA1 abrogated this change, indicating that decreased p62 was due to increased autophagic flux as expected (Fig. S3B).

In addition, MCF-7 cells stably transfected with GFP-LC3 exhibited a significant increase in punctate cytoplasmic structures (autophagic vesicles) when treated with NO (Fig. 3D). Autolysosomes are also called acidic vesicles, reflecting the presence of

acidic hydrolases that degrade vesicle contents (15). In response to NO, MCF-7 cells also showed an increase in acridine orange fluorescence associated with the presence of acidic vesicles and detected by flow cytometry (Fig. 3E).

Finally, Atg5<sup>+/+</sup> (autophagy-proficient) and Atg5<sup>-/-</sup> (autophagy-deficient) MEFs were used to confirm increased autophagy in response to NO (16). When cells of both types were treated with NO, increased LC3-II/LC3-I ratio and degradation of p62 occurred only in autophagy-proficient cells (Fig. 3F and G), indicating dependence on autophagy for the observed responses to NO. Importantly, Atg5<sup>+/+</sup> cells were more sensitive to NO-induced cell death, exhibiting >70% cell killing in response to low levels of NO (622  $\mu\text{M}\cdot\text{min}$ ), compared with autophagy-deficient cells, in which <20% loss in cell viability was induced by the same dose (Fig. 3H).

**NO Engages the ATM/LKB1/AMPK/TSC Signaling Pathway to Induce Autophagy.** Autophagy is an integral component of cellular damage responses to many types of stress, including nutrient deprivation, hypoxia, DNA damage, and oxidative stress. However, a mechanistic link between nitrosative stress and autophagy has not been described. Ataxia-telangiectasia mutated (ATM) is

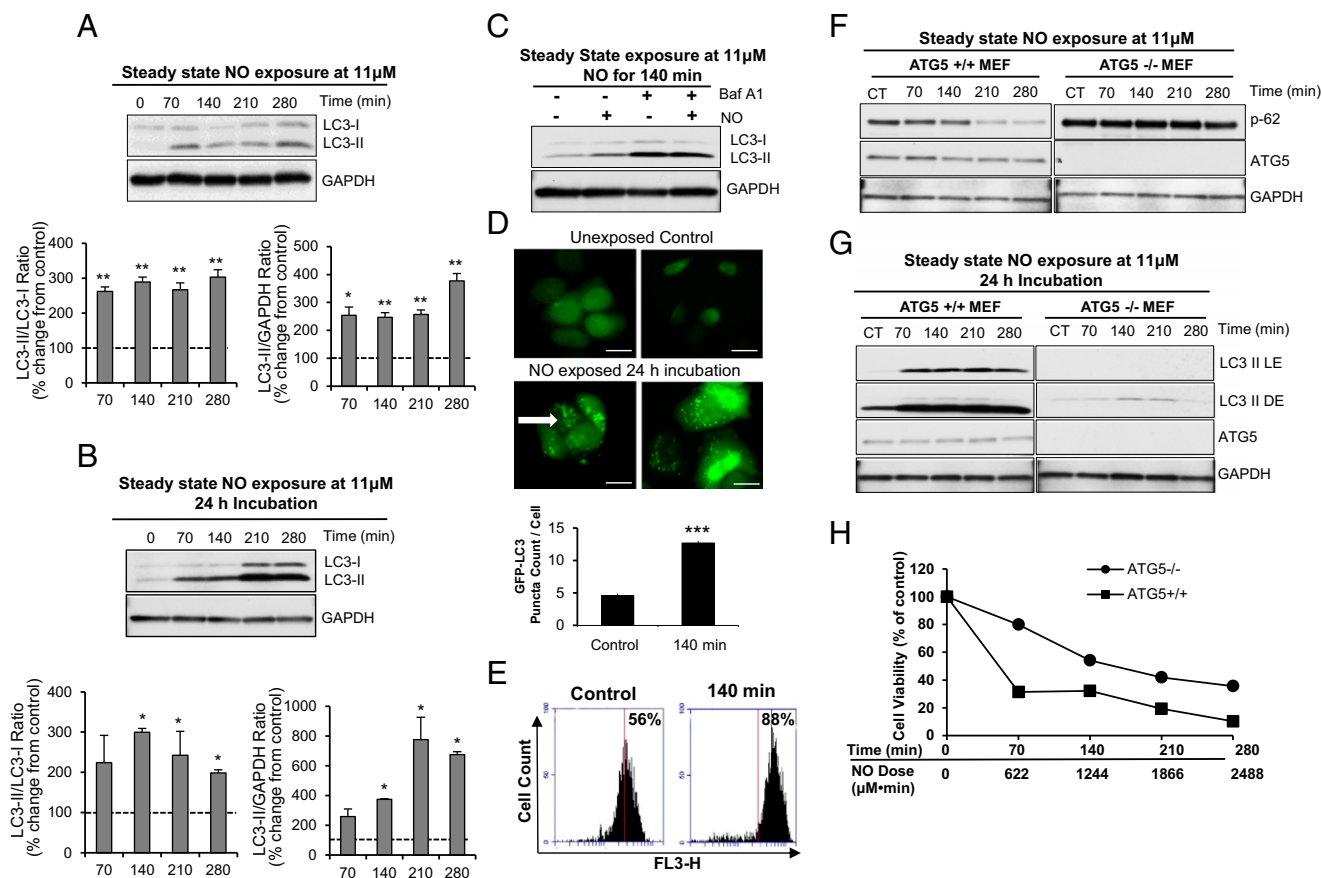


**Fig. 3.** Steady-state NO exposure leads to induction of autophagy. Western analysis with LC3 antibody shows (A) Increased ratio of LC3-II/LC3-I and LC3-II/GAPDH in NO-treated MCF-7 cells. The data are represented as mean  $\pm$  SD ( $n = 2$ ).  $^{**}P < 0.01$  and  $^{*}P < 0.05$  (a one-sample, one-sided  $t$  test). Horizontal dashed line indicates control values (100%). (B) The increased LC3-II persists during 24 h incubation post NO exposure in MCF-7 cells. The data are represented as mean  $\pm$  SD ( $n = 3$ ).  $^{*}P < 0.05$  (a one-sample, one-sided  $t$  test). Horizontal dashed line indicates control values (100%). (C) An increase in autophagic flux, as LC3-II increases in the presence of Bafilomycin A1 in NO-treated MCF-7 cells. (D) MCF-7 cells stably transfected with GFP-LC3 were exposed to NO at 11  $\mu\text{M}$  for 140 min and analyzed by microscopy after 24 h incubation for the presence of fluorescent GFP-LC3 puncta. Arrows identify puncta, and bar graph demonstrates a significant increase in their number. The data are represented as mean  $\pm$  SD ( $n = 3$ ).  $^{***}P < 0.001$  versus control (one-sided paired  $t$  test). (E) Flow cytometric analysis of acridine orange-stained autophagic vesicles induced by NO treatment. (F) Steady-state NO exposure induces autophagy in ATG5<sup>+/+</sup> but not ATG5<sup>-/-</sup> MEF. Western analysis shows degradation of p62 only in ATG5<sup>+/+</sup> cells. (G) Western analysis shows formation of autophagosome and increased LC3-II in ATG5<sup>+/+</sup> but not in ATG5<sup>-/-</sup> MEF. (H) Steady-state NO exposure leads to larger decrease in cell survival of ATG5<sup>+/+</sup> than in ATG5<sup>-/-</sup> MEF.

a key serine/threonine protein kinase that acts as a cellular damage sensor, coordinating the cell cycle with damage-response checkpoints and DNA repair machinery to maintain genomic integrity (17). Several well-known targets for the ATM kinase include p53 and CHK2, both of which become phosphorylated in response to reactive oxygen or nitrogen species (10, 18, 19). Moreover, ATM also functions as a damage sensor in the cytoplasm

via the recently described LKB1/AMPK/TSC pathway (10). Thus, we explored ATM and this downstream signaling pathway as a potential mechanism for NO signaling via mTORC1 and AMPK to induce autophagy.

Phosphorylation and activation of ATM (S1981) increased in cells under conditions of nitrosative stress in both the NO reactor (Figs. 2B and 4A), and in response to SN (Fig. S2C). Phosphorylation of

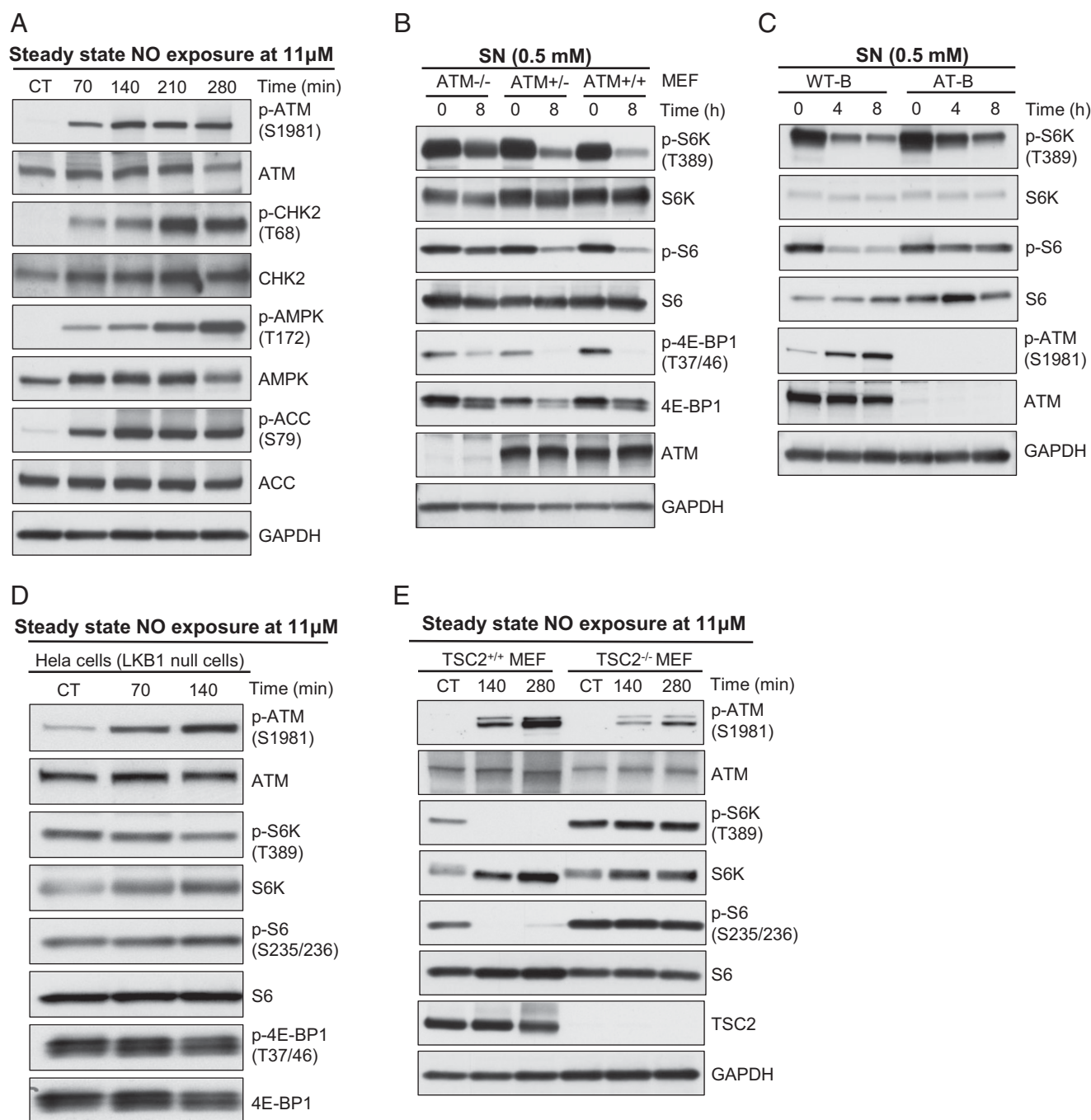


**Fig. 4.** Involvement of ATM signaling in mTORC1 repression following NO exposure. (A) Western analysis with p-ATM, p-CHK2, p-AMPK, and p-ACC antibodies and their total protein counterparts shows activation of ATM and downstream effectors in MCF-7 cells exposed to NO. (B) Western analysis of ATM<sup>+/+</sup>, ATM<sup>+/-</sup>, and ATM<sup>-/-</sup> MEF with p-S6K, p-S6, and p4E-BP1 antibodies shows that repression of mTORC1 by SN is ATM-dependent. (C) Western analysis of EBV-immortalized B-lymphocytes obtained from an AT (AT-B) patient and nonmutant individuals (WT-B) with p-ATM, p-S6K, and p-S6 antibodies shows that repression of mTORC1 by SN is ATM-dependent. (D) Western analysis with p-ATM, p-S6K, p-S6, and p4E-BP1 antibodies and their total protein counterparts in HeLa (LKB1-null cells) shows that repression of mTORC1 by NO exposure is LKB1-dependent. (E) Western analysis with p-ATM, p-S6K, and pS6 antibodies in TSC2<sup>+/+</sup> and TSC2<sup>-/-</sup> MEF shows that repression of mTORC1 by NO exposure is TSC2-dependent. CT, control.

Chk2 also increased concomitant with that of ATM, confirming activation of the ATM kinase (Fig. 4A). Importantly, in ATM-deficient MEFs (Fig. 4B and Fig. S4A) and ATM-deficient human lymphoblasts (Fig. 4C), mTORC1 repression and induction of autophagy in response to NO was greatly attenuated (Fig. 4B and C and Fig. S4A). Interestingly, as reported for ROS-induced activation of ATM, dependence on ATM for repression of mTORC1 was lost with adaptation of ATM-null cells to tissue culture (10). Taken together, these observations indicate that ATM plays a central role in mTORC1 repression and autophagy induction in response to nitrosative stress.

When activated by either DNA damage or oxidative stress, ATM phosphorylates LKB1, the Peutz-Jeghers syndrome tumor suppressor, at Thr366, activating this kinase and its downstream effector, AMPK (10, 20). Commensurate with ATM activation, we observed LKB1-dependent phosphorylation and activation of AMPK at T172 by nitrosative stress (Figs. 2B and 4A and Fig. S3C). AMPK activation was confirmed by phosphorylation of ACC at S79, a downstream target for the AMPK stress kinase (Fig. 4A and Fig. S3C). In contrast, as expected, mTORC1 repression and autophagy induction was not observed in LKB1-null HeLa cells under conditions of nitrosative stress (Fig. 4D and Fig. S4B). In addition to ACC, raptor was also phosphorylated by AMPK (Fig. 2B), suggesting that this inhibitory phosphorylation at S792 also contributed to mTORC1 repression.

An important downstream target of AMPK is the TSC2 tumor suppressor, a “gatekeeper” for mTORC1 signaling that suppresses mTORC1 in response to energy stress (5, 21). Using TSC2 proficient ( $TSC2^{+/+}$ ) and deficient ( $TSC2^{-/-}$ ) MEFs, we observed a dependence on TSC2 for mTORC1 repression and induction of autophagy in response to nitrosative stress (Fig. S4C). As shown in Fig. 4E, although ATM was activated in response to NO in both cell types, mTORC1 repression occurred only in TSC2-proficient cells, indicating a requirement for TSC2 in this response. Notably, both  $TSC2^{+/+}$  and  $TSC2^{-/-}$  MEFs are p53-deficient, indicating that p53 was not essential for repression of mTORC1 by NO.

The observed repression of mTORC1 and induction of autophagy described above is in contrast to a previous report from Sarkar et al., who, in 2011, reported that NO donors DETA NONOate and SIN-1 at high (500  $\mu$ M) doses induced the opposite responses, i.e., activated mTORC1 signaling and repressed autophagy in rat primary cortical neurons and HeLa cells (22). To investigate these discordant observations, we repeated our experiments under the same conditions used by Sarkar (22), using DETA NONOate as an NO source. HeLa cells were exposed to the NO donor for 24 h, during which medium and donor were replenished every 8 h. Under these conditions, we observed the same increase in mTORC1 signaling as reported by Sarkar (Fig. S3D). Given that cells were stimulated with medium containing serum every 8 h, we suggest the following possible explanations for the discordant findings: (i) increased nutrient load and activation of mitogenic signaling pathways stimulated mTORC1 activity, overriding the suppressive effects of NO; (ii) mTORC1 signaling was evaluated only at 24 h; thus, rapid, early effects that we observe at 2–8 h after treatment with NO donor would be missed; (iii) changing the medium every 8 h would remove those reactive nitrogen species formed in response to the NO donor, which are more toxic than NO itself; and (iv) HeLa cells used for their studies are LKB1-deficient, which, as we show above, abrogates the ability of ATM to signal to LKB1 to activate AMPK and TSC to repress mTORC1.

Taken together, our data suggest a model (Fig. 5) whereby nitrosative stress engages the ATM kinase to activate LKB1, AMPK, and TSC2. As a result of TSC2 activation, and possibly direct phosphorylation of raptor by AMPK, mTORC1 is repressed. The combined loss of (repressive) phosphorylation of ULK1 and increased (activating) phosphorylation of ULK1 by AMPK results

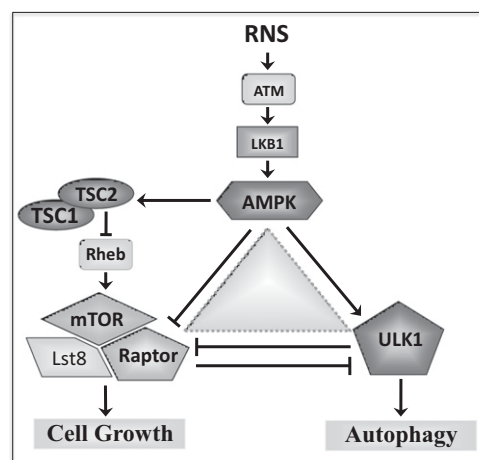


**Fig. 5.** Schematic diagram depicting pathway through which NO and RNS engage ATM to activate AMPK via LKB1 and repress mTORC1 to modulate ULK1 activity and induce autophagy.

in increased autophagy and autophagy-mediated cell death in response to nitrosative stress.

## Discussion

NO is a key signaling molecule that mediates numerous physiological and pathological processes, depending upon concentration, cell type, cellular environment, exposure duration, proximity (intracellular or extracellular), and source. We found that exogenous exposure to NO rapidly activated ATM kinase, a damage response protein that recognizes DNA damage in the nucleus and oxidative damage in the cytoplasm. Activated ATM signals to AMPK, and we observed a dependence on LKB1 for activation of AMPK and repression of mTORC1 in response to NO, as previously reported for ROS (10). Both ROS and RNS damage DNA and trigger ATM activation to repair this DNA damage. However, whereas ROS has been shown to activate cytosolic ATM, additional studies are required to determine whether nitrosative stress activates ATM in the cytoplasm, nucleus, or both.

At present, the precise biochemical mechanism of activation of ATM in response to nitrosative stress is not clear. ATM is a very large protein (~350 kDa) containing many cysteine residues. Recently, Paull and coworkers reported that, in response to ROS, ATM is directly activated via oxidation of cysteine residue(s) and formation of an active ATM homodimer (23). NO may similarly cause conformational changes in ATM via nitrosylation of sulfhydryl or oxidation of sulfhydryl groups by interaction with RNS reactive intermediates leading to formation of active ATM dimers (23). However, further work is needed to determine the precise mechanism of ATM activation in response to nitrosative stress.

In our studies, we used both a reactor in which cells were exposed to steady-state NO and an NO donor (SN) and observed mTORC1 repression and induction of autophagy under both conditions. The role of nitrosative stress in regulating mTORC1 signaling and autophagy has not previously been extensively explored. We have identified several kinases, including ATM, AMPK, and LKB1, that participate in a nitrosative-stress signaling cascade via the tumor suppressors LKB1 and TSC2, which act to repress mTORC1. Although ATM appears to suppress mTORC1 via LKB1, AMPK may contribute to mTORC1 repression both directly, by phosphorylating raptor, and indirectly, via activation of TSC2 (Fig. 5). Our data indicate that the engagement of the ATM/LKB1/AMPK/TSC2 signaling cascade by nitrosative stress functions primarily to repress mTORC1 and induce autophagy.



Autophagy is a dichotomous phenomenon, involved in cell survival as well as cell death, depending upon both magnitude and cell context. Autophagy can promote cell survival by removing old or damaged cellular organelles and recycling key cellular building blocks for use in required metabolic pathways and construction of macromolecules. Cancer cells frequently use autophagy to survive nutrient deprivation induced by therapeutic agents. However, autophagy above a certain threshold can also induce cell death and, if triggered appropriately, can be used as a means of killing cancer cells. Interestingly, our data, showing that cell viability decreased in the presence of NO and that  $ATG5^{+/+}$  cells were more sensitive to NO cytotoxicity than  $ATG5^{-/-}$  cells, suggest that autophagy is a prodeath response to nitrosative stress. Originally designated as type-II programmed cell death, autophagy can be a major death mechanism in cells that are resistant to apoptosis, as in settings of elevated BCL-2 activation or caspase-3 deficiency (24, 25). Breast cancer cells such as MCF-7 possess both of these properties and are resistant to apoptosis (26, 27). If these and other types of cancer cells are indeed particularly sensitive to induction of autophagy by nitrosative stress, this sensitivity suggests an opportunity to take advantage for designing cancer therapies that use nitrosative stress to induce cancer cell death. Future additional experiments to characterize the therapeutic index of “nitrosative stress therapy” may yield new insights into how to best exploit this phenomenon to develop more effective cancer therapies.

## Materials and Methods

**Cell Culture, Antibodies, and Reagents.** MCF-7 cells [American Type Culture Collection (ATCC)] were grown in Improved Modified Eagle's Medium (IMEM) supplemented with 10% (vol/vol) FBS and cultured in a humidified incubator at 37 °C with 5% CO<sub>2</sub>. MCF-7 cells stably expressing GFP-LC3 were maintained in RPMI 1640 supplemented with 10% (vol/vol) FBS.  $TSC2^{+/+}$  and  $TSC2^{-/-}$  Mouse Embryonic Fibroblasts (MEFs) (kind gifts from Dr. D. Kwiakowski, Harvard Medical School, Boston, MA) and HeLa cells (ATCC) were grown in MEM supplemented with 10% FBS.  $ATM^{+/+}$  human lymphoblasts (GM02184) and  $ATM^{-/-}$  human lymphoblasts (GM01526) were acquired fresh (from Coriell Repositories) for each experiment and maintained in RPMI 1640 supplemented with 15% FBS for less than four passages in culture. Primary fibroblast  $ATM^{+/+}$ ,  $ATM^{+/-}$ , and  $ATM^{-/-}$  cells derived from embryos at gestation day 13 were maintained in DMEM media with 15% FBS. Anti-S6K, anti-phospho-S6K (Thr389), anti-S6, anti-phospho-S6 (Ser235/236), anti-4E-BP1, anti-phospho-4E-BP1 (Thr37/46), anti-phospho-CHK2 (Thr68), anti-p53, anti-phospho-p53 (Ser15), anti-AMPK, anti-phospho-AMPK (Thr172), anti-ACC, anti-phospho-ACC (Ser79), and anti-LC3 were purchased from Cell Signaling Technologies. Other antibodies used were anti-ATM (GeneTex), anti-TSC2 (Epitomics), anti-phospho-ATM (Ser1981) (Epitomics), and GAPDH and HRP-conjugated secondary antibodies were obtained from Santa Cruz Biotechnology. Nitric oxide donor spermine NONOate was purchased from Cayman Chemical. Caspase Inhibitor Z-VAD-FMK was purchased from Promega, Necroptotic inhibitor Necrostatin-1, and Emodin were purchased from SIGMA, and Staurosporine was obtained from LC Laboratory.

**NO Exposure.** Cells cultured at a density of 70–80% confluence were plated in 60-mm dishes 24 h before exposure to NO. Using the NO-delivery system described elsewhere (28, 29), equipped to maintain NO at steady-state concentration, cells were exposed to 11  $\mu$ M NO for the indicated time points to produce the following cumulative doses: 622  $\mu$ M•min (70 min); 1,244  $\mu$ M•min (140 min); 1,866  $\mu$ M•min (210 min); and 2,488  $\mu$ M•min (280 min). Cells exposed to 5% CO<sub>2</sub>:21% O<sub>2</sub>:74% N<sub>2</sub> served as controls. Gases were purchased from Airgas. Cells were harvested to prepare cell lysates using the RIPA protocol at various times postexposure (see *Immunoblotting*).

**Treatment with Spermine NONOate and DETA NONOate.** MCF-7 cells at ~70% confluency were treated with 0.5 mM Spermine NONOate (SN), and lysate was prepared at different time intervals. Cells were treated with the NO donor DETA NONOate (DN), for 24 h, during which medium containing fresh donor compound was replenished every 8 h. For cytotoxicity determination, MCF-7 cells were treated with 0.5 mM, 1 mM and 2 mM spermine NONOate with or without caspase inhibitor Z-VAD-FMK (20  $\mu$ M) or programmed necrosis inhibitor Necrostatin-1 (NEC1, 10  $\mu$ M). Z-VAD-FMK and NEC1 were added 1 h before spermine NONOate treatment. After 24 h incubation, cell

viability was performed by WST-1 assay (Roche) as described by manufacturer protocol. Emodin at the dose of 20  $\mu$ M and staurosporine at the dose of 1  $\mu$ M serve as a positive control.

**NO Exposure and Bafilomycin A1 Treatment.** Cells were cultured as above. One hour before exposure to NO, cells were pretreated with 200 nM Bafilomycin A1 in DMSO 3  $\mu$ L/3 mL or 0.1% DMSO. Treated plates were placed in reactors that contained IMEM with 200 nM Bafilomycin or IMEM with 0.1% DMSO and treated with NO or 5% CO<sub>2</sub>:21% O<sub>2</sub>:74% N<sub>2</sub> as a control. Cells were harvested immediately after exposure, and cell lysates were made using RIPA protocol (see *Immunoblotting*).

**Cell Viability Analysis.** Cell viability was analyzed by WST-1 assay following the manufacturer's protocol (Roche). Briefly, coverslips on which  $1 \times 10^4$  cells had been grown overnight in 24-well plates were transferred to specially modified NO delivery reactors and exposed to 11  $\mu$ M NO for specified time periods, after which they were transferred to 24-well plates containing 300  $\mu$ L of fresh medium. After 24 h of incubation, 30  $\mu$ L of WST-1 per well was added to the medium followed by incubation for 1 h at 37 °C for 1 h and measurement of absorbance at 490 nm (Spectra Max Gemini; Molecular Device). Absorbance directly correlated with the number of metabolically active cells in the culture, and cell survival was expressed as a percentage of control cell viability.

**Immunoblotting.** Following NO exposure, cells were washed twice with PBS and harvested in RIPA buffer (Sigma-Aldrich) plus 1 mM phenylmethylsulfonyl fluoride (PMSF), 1 mM sodium orthovanadate (Na<sub>3</sub>VO<sub>4</sub>), 1 mM sodium fluoride (NaF), and protease mixture inhibitor. The cells were rocked for 30 min at 4 °C and then centrifuged at 10,000  $\times$  g for 10 min. Protein concentrations were measured by Pierce BCA protein assay kit. Before loading, samples were mixed with an equal volume of Laemmli Sample Buffer (Bio-Rad), heat denatured (100 °C, 10 min) with  $\beta$ -mercaptoethanol ( $\beta$ -ME; Sigma-Aldrich), loaded in precast SDS/PAGE gels (Bio-Rad), transferred to nitrocellulose membranes, and probed with specific primary antibodies overnight at 4 °C: primary antibody p-ATM (S1981) antibody (1:1,000 dilution), ATM antibody (1:1,000 dilution), p-AMPK (T172) antibody (1:500 dilution), AMPK antibody (1:500), p-ACC (S-79) antibody (1:1,000 dilution), ACC antibody (1:1,000 dilution), p-S6K (T389) antibody (1:500 dilution), S6K antibody (1:500 dilution), p-S6 (S235/236) antibody (1:2,000 dilution), S6 antibody (1:2,000 dilution), p-4E-BP-1 (T37/46) antibody (1:2,000 dilution), 4E-BP-1 antibody (1:2,000 dilution), p-CHK2 (T68) antibody (1:1,000 dilution), CHK2 antibody (1:1,000 dilution), and LC3 antibody (1:1,000 dilution). The following day, they were probed with secondary anti-mouse or anti-rabbit IgG conjugated horseradish peroxidase antibody, and chemiluminescence was detected. As a protein loading control, membranes were stripped and reprobed with GAPDH antibody (1:5,000 dilution).

**GFP-LC3 Localization.** MCF-7 cells stably transfected with GFP-LC3 construct were plated on coverslips and exposed to nitric oxide in the NO delivery system. The cells were then fixed in 4% paraformaldehyde for 15 min at room temperature. Coverslips were mounted using Ultra Cruz Mounting Medium and examined in a Nikon Eclipse E600 fluorescence microscope for presence of autophagic puncta. The number of puncta per cell was determined and data were expressed as number of puncta per cell compared with unexposed GFP positive control or cells exposed to control gas.

**Acidic Vesicle Detection.** Detection and quantification of acidic vesicle formation during the process of autophagy was performed by acridine orange staining followed by flow cytometric analysis. In brief, MCF-7 cells were exposed to NO in the delivery system, incubated for 24 h in the incubator, harvested by trypsinization, washed twice with PBS, and then stained with acridine orange at a final concentration of 1  $\mu$ g/ $\mu$ L for 30 min in the dark. Acridine orange is a weak base that can accumulate in acidic compartments, emitting bright red fluorescence, the intensity of which is proportional to the degree of acidity and/or volume of the compartment. Samples were then processed by flow cytometry using blue laser and 620/20 (AO-red) and 530/30 (AO-green) filters in a C6-Accuri Flow Cytometer.

**Detection of Apoptosis.** For determination of rate of apoptosis, cells were cultured as described above and exposed to NO (steady-state 11  $\mu$ M) for various lengths of time, followed by 24 h incubation in a humidified incubator with 5% CO<sub>2</sub>. Apoptosis was assessed by ApoAlert annexinV-FITC (fluorescein isothiocyanate) and propidium iodide (PI) apoptosis kit (Clontech) according to the manufacturer's instructions. Briefly, cells were collected,



washed with PBS, resuspended in binding buffer provided, and stained with annexinV (5  $\mu$ L) and PI (10  $\mu$ L), and fluorescence was measured on a C6-Accuri Flow Cytometer.

**Detection of PARP.** MCF-7 cells were treated as above in the NO delivery system. Samples and matched controls were harvested at times 0, 24, 48, and 72 h posttreatment as follows. At 0 h, all cells were collected from the reactor supernatant and PBS washed by centrifugation for 5 min at 1,200 rpm. Lysis buffer (15  $\mu$ L) was added to the pellet and added to the lysis buffer recovered from the cell culture dish. Samples were then treated as described in *Immunoblotting*. Medium and washes collected from time points 24, 48, and 72 h were centrifuged and added to the lysis buffer collected from the cell culture dishes. In this process, all cells living and dead are collected and processed for PARP cleavage determination.

**Statistical Methods.** All data are represented as mean  $\pm$  SD. The statistical analysis was performed by SAS statistical software. The quantitative analysis of Western data was represented as the percentage of fold change from

control. Using this fold-change value, a one-sample, one-sided *t* test was performed to determine whether the percent change from control was higher than 100%. This same method was used for each experiment examining LC3-II with the respective controls. Similarly, fold change in p62 was calculated and was analyzed with a one-sample, one-sided *t* test to determine whether the fold change was less than 100%. The GFP-LC3 puncta count was compared between control and NO treated group using a one-sided paired *t* test. Any *P* values less than 0.05 were considered statistically significant.

**ACKNOWLEDGMENTS.** We thank Dr. Gordon Mills and Yiling Lu (University of Texas M. D. Anderson Cancer Center) for providing the MCF-7 cell line stably expressing GFP-LC3, and we thank RIKEN BRC for ATG5<sup>+/+</sup> MEF and ATG5<sup>-/-</sup> MEF cells. We thank Tia Berry, Tong Xuefei, and Ji Jing (Institute for Biosciences and Technology, Texas A&M Health Science Center) for technical help, Elaine Dunlop (Cardiff University, UK) for assessing reproducibility of our data, and Dr. Luiz C. Godoy (Massachusetts Institute of Technology) for insightful discussions. This work was supported by National Institutes of Health Grants RO1 CA143811, 5 P01 CA26731, and ES002109.

1. Baehrecke EH (2005) Autophagy: Dual roles in life and death? *Nat Rev Mol Cell Biol* 6(6):505–510.
2. Codogno P, Meijer AJ (2005) Autophagy and signaling: Their role in cell survival and cell death. *Cell Death Differ* 12(Suppl 2):1509–1518.
3. Levine B, Yuan J (2005) Autophagy in cell death: An innocent convict? *J Clin Invest* 115(10):2679–2688.
4. Aleem E, Kiyokawa H, Kaldis P (2005) Cdc2-cyclin E complexes regulate the G1/S phase transition. *Nat Cell Biol* 7(8):831–836.
5. Inoki K, Zhu T, Guan KL (2003) TSC2 mediates cellular energy response to control cell growth and survival. *Cell* 115(5):577–590.
6. Wullschlegel S, Loewith R, Hall MN (2006) TOR signaling in growth and metabolism. *Cell* 124(3):471–484.
7. Kim J, Kundu M, Viollet B, Guan KL (2011) AMPK and mTOR regulate autophagy through direct phosphorylation of Ulk1. *Nat Cell Biol* 13(2):132–141.
8. Thomas DD, et al. (2008) The chemical biology of nitric oxide: Implications in cellular signaling. *Free Radic Biol Med* 45(1):18–31.
9. Xu W, Liu LZ, Loizidou M, Ahmed M, Charles IG (2002) The role of nitric oxide in cancer. *Cell Res* 12(5-6):311–320.
10. Alexander A, et al. (2010) ATM signals to TSC2 in the cytoplasm to regulate mTORC1 in response to ROS. *Proc Natl Acad Sci USA* 107(9):4153–4158.
11. Mizushima N (2010) The role of the Atg1/ULK1 complex in autophagy regulation. *Curr Opin Cell Biol* 22(2):132–139.
12. Ganley IG, et al. (2009) ULK1.ATG13.FIP200 complex mediates mTOR signaling and is essential for autophagy. *J Biol Chem* 284(18):12297–12305.
13. Kuma A, Matsui M, Mizushima N (2007) LC3, an autophagosome marker, can be incorporated into protein aggregates independent of autophagy: Caution in the interpretation of LC3 localization. *Autophagy* 3(4):323–328.
14. Tanida I, Ueno T, Kominami E (2008) LC3 and Autophagy. *Methods Mol Biol* 445:77–88.
15. Paglin S, et al. (2001) A novel response of cancer cells to radiation involves autophagy and formation of acidic vesicles. *Cancer Res* 61(2):439–444.
16. Kuma A, et al. (2004) The role of autophagy during the early neonatal starvation period. *Nature* 432(7020):1032–1036.
17. Kastan MB, Bartek J (2004) Cell-cycle checkpoints and cancer. *Nature* 432(7015):316–323.
18. Alexander A, Walker CL (2010) Differential localization of ATM is correlated with activation of distinct downstream signaling pathways. *Cell Cycle* 9(18):3685–3686.
19. Goodman JE, Hofseth LJ, Hussain SP, Harris CC (2004) Nitric oxide and p53 in cancer-prone chronic inflammation and oxyradical overload disease. *Environ Mol Mutagen* 44(1):3–9.
20. Alessi DR, Sakamoto K, Bayascas JR (2006) LKB1-dependent signaling pathways. *Annu Rev Biochem* 75:137–163.
21. Hardie DG (2004) The AMP-activated protein kinase pathway—new players upstream and downstream. *J Cell Sci* 117(Pt 23):5479–5487.
22. Sarkar S, et al. (2011) Complex inhibitory effects of nitric oxide on autophagy. *Mol Cell* 43(1):19–32.
23. Guo Z, Kozlov S, Lavin MF, Person MD, Paull TT (2010) ATM activation by oxidative stress. *Science* 330(6003):517–521.
24. Dalby KN, Tekedereli I, Lopez-Berestein G, Ozpolat B (2010) Targeting the prodeath and prosurvival functions of autophagy as novel therapeutic strategies in cancer. *Autophagy* 6(3):322–329.
25. Levine B (2007) Cell biology: Autophagy and cancer. *Nature* 446(7137):745–747.
26. Buchholz TA, et al. (2003) Chemotherapy-induced apoptosis and Bcl-2 levels correlate with breast cancer response to chemotherapy. *Cancer J* 9(1):33–41.
27. Devarajan E, et al. (2002) Down-regulation of caspase 3 in breast cancer: A possible mechanism for chemoresistance. *Oncogene* 21(57):8843–8851.
28. Li CQ, et al. (2009) Nitric oxide activation of Keap1/Nrf2 signaling in human colon carcinoma cells. *Proc Natl Acad Sci USA* 106(34):14547–14551.
29. Wang C, Deen WM (2003) Nitric oxide delivery system for cell culture studies. *Ann Biomed Eng* 31(1):65–79.